Available online at www.sciencedirect.com

ScienceDirect

Energy Procedia 38 (2013) 101 – 107

Energy Procedia

SiliconPV: March 25-27, 2013, Hamelin, Germany

Classification of defective regions in *p*-type multicrystalline silicon by comparing luminescence images measured under different conditions

Rafael Krain[a]*, Svetlana Beljakova[b], Sandra Herlufsen[a], Michael Krieger[b], Jan Schmidt[a]

[a]*Institute for Solar Energy Research Hamelin (ISFH), Am Ohrberg 1, 31860 Emmerthal, Germany*
[b]*Lehrstuhl für Angewandte Physik, Friedrich-Alexander-University Erlangen-Nürnberg (FAU), Staudtstrasse 7, 91058 Erlangen, Germany*

Abstract

In this contribution, we apply three different camera-based luminescence imaging techniques to mc-Si wafers and solar cells, fabricated on neighboring wafers. On wafer level, we determine the spatially-resolved carrier lifetime using calibrated photoluminescence lifetime imaging. On the solar cell level, we use band-to-band electroluminescence and sub-band-gap electroluminescence imaging for the characterisation. We analyze the differences obtained by the different techniques in specific defective areas. Characteristic regions are additionally examined using deep-level transient spectroscopy (DLTS). Comparing different luminescence images, we find different signal correlations in selected regions of the wafers and the neighboring cells presumably caused by different types of defects, which react more or less effective on the phosphorus gettering during the solar cell process. DLTS spectra show that in the edge region of the wafer close to the crucible, FeB pairs are present in the wafer as well as in the cell. However, the FeB concentration in the cell is, due to phosphorus gettering during the cell process, reduced by one order of magnitude. In regions which appear as very recombination-active defect clusters in the solar cell, we detect ZnB pairs by DLTS analysis. Note that the ZnB itself is a shallow centre and therefore expected to be not strong recombination active. However, our measurements reveal that Zn is present in regions with increased recombination activity, which is also in good agreement with the high total Zn concentration measured in the mc-Si ingot. We hence conjecture that dislocation clusters decorated by Zn are responsible for the non-getterable defect regions.

* Corresponding author. Tel.: +49-5151-999637; fax: +49-5151-999600
E-mail address: krain@isfh.de

doi:10.1016/j.egypro.2013.07.255

Keywords: defects; luminescence; multicrystalline silicon; DLTS; FeB; ZnB;

1. Introduction

Multicrystalline silicon (mc-Si) used in the production of solar cells contains high densities of crystallographic defects such as dislocation clusters, and grain boundaries as well as impurities such as metals and oxygen. Although many harmful, i.e. recombination-active, impurities, in particular metals, can be very effectively gettered, a considerable fraction of them is still present in solar cells and may reduce the carrier diffusion length considerably. A typical situation leading to reduced gettering efficiency is if metals are attached to crystallographic defects.

In the last years, camera-based luminescence imaging methods have been developed and have been proven to allow a fast spatial characterization of silicon wafers and solar cells. For the characterisation on the wafer level, photoluminescence (PL) imaging [1] has been developed, which allows the contactless investigation of Si wafers since the excess carriers are optically generated. On the solar cell level, electroluminescence (EL) images are generated by electrically injecting excess carriers into the cell [2]. More recently, the detection of sub-band-gap luminescence (SBG-EL) has been demonstrated to be capable of providing additional information [3].

2. Experimental

We examine wafers from the middle region of a boron-doped mc-Si ingot with a resistivity of 1 Ωcm. The wafers are passivated with aluminum oxide (Al_2O_3) grown by thermal atomic layer deposition, which implies very low surface recombination velocities below 10 cm/s [4]. The deposition temperature was 260 °C and the samples were annealed in atmosphere at 350 °C to activate the surface passivation. For the spatially resolved lifetime mappings, we use a photoconductance-calibrated photoluminescence lifetime imaging (PCPLI) setup [5]. The excitation of excess carriers is performed by means of a laser at a central wavelength of 808 nm and the emitted luminescence radiation is detected using a Si-CCD camera.

Solar cells are processed on neighboring wafers using an industrial screen-printing cell process. The solar cells are characterized using camera-based electroluminescence measurements [6]. In this case, excess carriers are injected into the cell's base by the application of a forward-bias voltage. The band-to-band electroluminescence emission is detected by a Si-CCD camera. Through the installation of long-pass-filters, which block the radiation with wavelengths below the band-gap wavelength of silicon, and replacing the Si-CCD camera with an InGaAs-camera, sub-band-gap EL measurements are realized.

In addition to the camera-based luminescence techniques, we analyze selected regions of the wafers and the cells by means of deep level transient spectroscopy (DLTS) using a PhysTech DLTS system [7]. For these measurements, circular Ti/Al Schottky contacts have been deposited onto the front side of selected pieces of the wafer, and a large-area Al ohmic contact was used on the backside. On the processed cells, MESA diodes have been fabricated by reactive ion etching after removing the original solar cell contacts. The diodes have been contacted by ohmic Al contacts. For the investigated samples, the DLTS detection limit for point defects was 1×10^{11} cm^{-3}.

3. Results

Figure 1 shows three representative luminescence images recorded by the three different techniques of a neighboring wafer and solar cell (a: PL, b: EL, c: SBG EL). The colored circles and ellipses represent regions, which show different correlations related to the detected luminescence signals using PL, EL and SBG EL imaging.

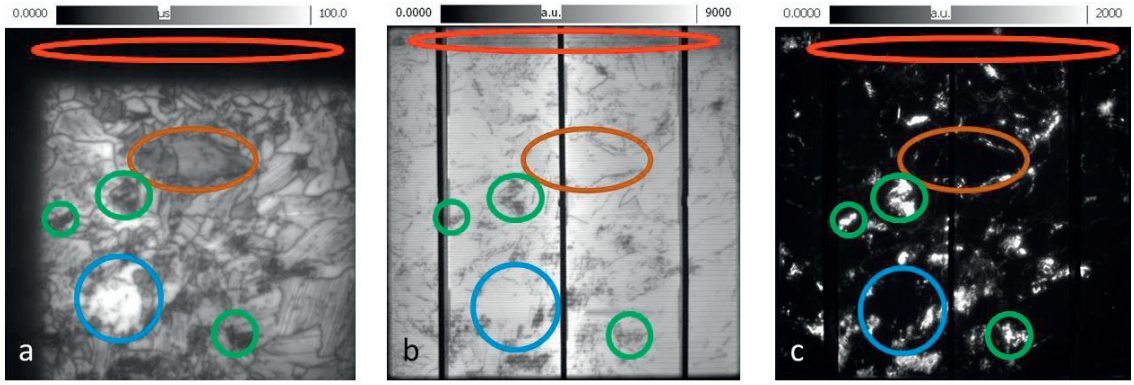

Fig. 1. (a) PL, (b) EL and (c) SBG-EL images of neighboring wafers and cells from the middle of an mc-Si ingot.

The region marked by a blue circle represents a region with a high carrier lifetime, i.e. a high PL signal, a high EL signal and an absent SBG EL signal. Apparently, in this region the concentration of metallic impurities as well as the dislocation density is already very low after the crystallization process. This assumption is in good agreement with the results from a DLTS analysis which was performed in the blue-circled region of Fig. 1. Figure 2 shows the DLTS spectra taken on a wafer and a solar cell in this region. The DLTS spectrum measured on the wafer shows no defect peaks, whereas the measurement performed on the solar cell shows a broad distribution of peaks. As it will be also shown in Figs. 3 to 5, this ‘broad structure’ is independent of the recombination activity of the examined region, as it was observable in all examined samples from different regions. In addition the spectrum of the ‘broad structure’ is not affected by the pulse voltage (forward or reverse). We assume that the broad structure results from the interface states located at the MESA edges created during the reactive ion etching process. Further investigations are required to fully understand the physical origin of the unexpected negative DLTS signal.

One frequently found correlation is marked by green circles in Fig. 1. For this type of defects, a low-lifetime region in the PL lifetime image correlates with a low EL signal and a high SBG EL signal on the solar cell fabricated on a neighboring wafer. The recombination activity of these regions is probably dominated by metal-decorated crystallographic defects (in particular dislocation clusters), which could not be effectively gettered during the solar cell process. Our comparative measurements hence suggest that metal-decorated dislocations lead to a pronounced SBG EL signal. Figure 3 shows the DLTS spectrum of one of these green-circled regions. In addition to the discussed broad structure measured in all investigated cell samples, the wafer as well as the cell show a pronounced DLTS peak at very low temperature. Due to the DLTS signature of the peak, which implies a peak temperature at 45 K, an ionization energy of 88 meV, and a hole capture cross section of 6.1×10^{-14} cm^2, we attribute this peak to the ZnB (zinc-boron) pair [8]. This finding is consistent with ICP-MS (inductively-coupled plasma mass

spectrometry) measurements, where Zn concentrations of about 10^{14} cm^{-3} had been found in this block. The ZnB concentration found in one of the green-circled regions (wafer and cell) is about 3×10^{12} cm^{-3}. These results suggest that Zn-decorated dislocation clusters, which are not directly observable by DLTS, might at least partly be causing the high recombination activity in the green-circled region of Fig. 1.

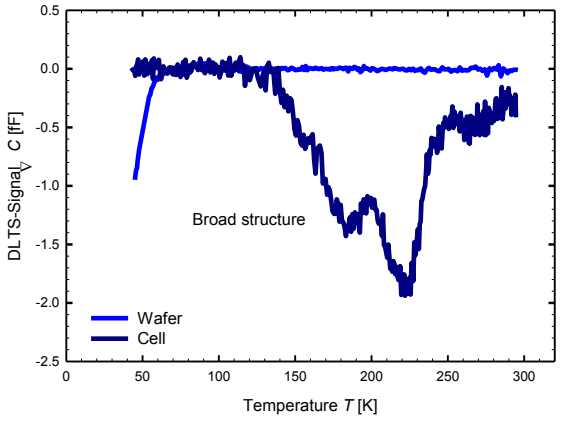

Fig. 2. DLTS spectrum of the region marked by a blue circle in Fig. 1, showing a high PL and EL signal and no SBG EL signal.

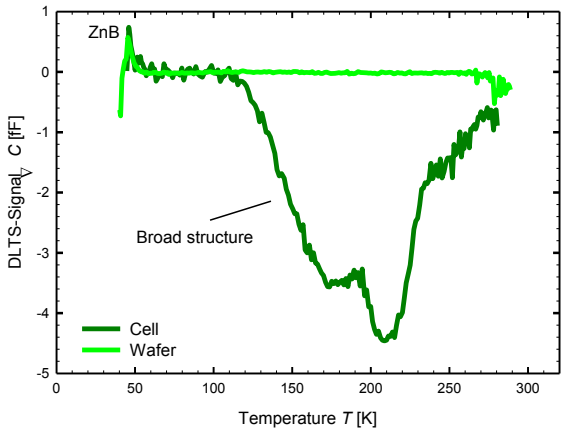

Fig. 3. DLTS spectrum of a region marked with a green circle in Fig. 1, showing a weak PL and EL signal and a high SBG EL signal.

In contrast to the regions marked with the green circles, the area marked with a brown ellipse in Fig. 1 shows a low lifetime in the PL image, however, after processing we find in the same region an increased EL signal and no SBG EL signal. We assume that such regions contain high concentrations of metallic impurities after crystallization and relatively low densities of crystallographic defects. During the solar cell process, the mobile metallic impurities are effectively phosphorus-gettered and, hence, do not affect the solar cell properties. Figure 4 shows the DLTS signal of this region (wafer and cell). In the cell DLTS sample, we merely observe the broad structure discussed above. In the wafer sample, we observe a DLTS

peak corresponding to a defect concentration of 2×10^{12} cm^{-3}. This peak shows the same DLTS signature as discussed above and can be assigned to the ZnB pair.

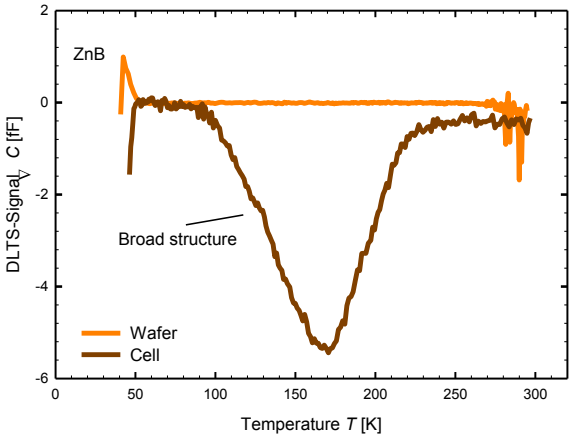

Fig. 4. DLTS spectrum of the region marked with the brown ellipse in Fig. 1, showing a weak PL signal, a high EL signal, and no SBG EL signal.

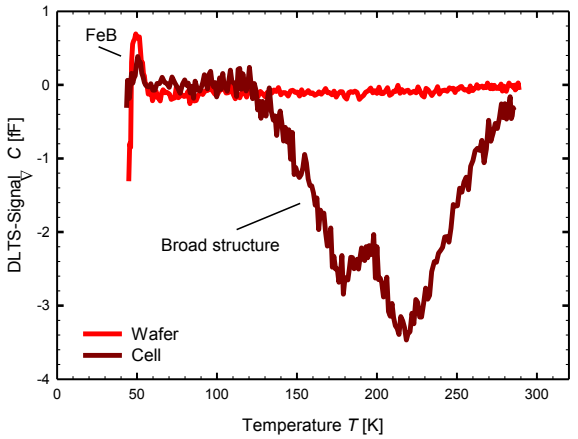

Fig. 5. DLTS spectrum of the edge region marked with a red ellipse in Fig. 1, showing no PL signal, a moderate EL signal, and no SBG EL signal.

The border region marked with a red ellipse in Fig. 1 shows another typical correlation. This region contains a high concentration of metallic impurities diffused from the crucible wall into the silicon during the crystallization of the ingot. The extremely high impurity concentration in this region reduces the lifetime to below 2µs. Phosphorus gettering cleans the region, however, the EL image shown in Fig. 1 (b) shows a slightly reduced signal compared to the averaged EL signal over the complete cell area. Interestingly, we measure no SBG EL signal in this low-lifetime edge region. From this finding one might conclude that the edge regions do not have an increased dislocation density. Comparing this to the DLTS

spectra shown in Fig. 5 we observe that in the wafer as well as in the corresponding cell a DLTS-detectable defect is present. Due to the DLTS peak temperature of 52 K, an ionization energy of 102 meV, and a hole capture cross section of 9.2×10^{-14} cm^2, this peak can be attributed to the FeB (iron-boron) pair [9]. According to ICP-MS measurements of the same mc-Si ingot, total iron concentrations up to 7×10^{14} cm^{-3} are present in the ingot. While the FeB concentration in the edge region of the wafer is 6×10^{12} cm^{-3}, after the phosphorus gettering during the cell process the concentration is reduced by one order of magnitude to 5×10^{11} cm^{-3}.

Table 1 summarizes the results of our luminescence and DLTS measurements.

4. Conclusions

We have presented a classification of the luminescence signals of different regions of mc-Si wafers and solar cells using different luminescence imaging techniques, namely PL imaging on surface-passivated mc-Si wafers and band-to-band EL imaging and sub-band-gap EL imaging on solar cells fabricated on neighbouring wafers. The different luminescence signal correlations are probably caused by different types of defects, which react more or less effective on the phosphorus gettering during the solar cell process. Comparing these correlations with DLTS data we find regions with no evidence of majority carrier trapping centers at all. In other regions FeB-pairs are detected by DLTS, with a significant concentration also detectable after cell processing, i.e. after phosphorus gettering. In regions which show a pronounced sub-band-gap luminescence and a pronounced recombination activity on wafer and cell level, a DLTS peak is found at very low temperature, which we attribute to the ZnB pair. Interestingly, in some cell regions, ZnB could be eliminated by the phosphorous gettering process, while in other regions, a clear ZnB peak is observed in DLTS even after cell processing.

Table 1. Summary of the results from the luminescence and DLTS measurements on different defective regions of the mc-Si wafer and the neighbouring solar cell shown in Fig. 1.

region	PL signal	EL signal	SBG-EL signal	FeB_{wafer} [cm^{-3}]	FeB_{cell} [cm^{-3}]	ZnB_{wafer} [cm^{-3}]	ZnB_{cell} [cm^{-3}]
blue	high	high	-----	-----	-----	-----	-----
green	weak	weak	high	-----	-----	3×10^{12}	3×10^{12}
brown	weak	high	-----	-----	-----	2×10^{12}	-----
red	low	mean	low	6×10^{12}	5×10^{11}	-----	-----

Acknowledgments

This work was financially supported by the German Federal Ministry for the Environment, Nature Conservation and Nuclear Safety and by industry partners within the research cluster “SolarWinS” (contract No. 0325270E). The content is the responsibility of the authors. We thank Sylke Meyer from Frauenhofer CSP for ICP-MS measurements and Daniel Reinke of Sunways AG for the solar cell processing.

References

[1] T. Trupke, J. Nyhus, and J. Haunschild, Luminescence imaging for inline characterization in silicon photovoltaics, *Physica Status Solidi (RRL)*, **5(4)**, (2011) pp. 131-137

[2] T. Fuyuki, H. Kondo, Y. Kaji, T. Yamazaki, Y. Takahashi, and Y. Uraoka, ONE SHOT MAPPING OF MINORITY CARRIER DIFFUSION LENGTH IN POLYCRYSTALLINE SILICON SOLAR CELLS USING ELECTROLUMINESCENCE, *Proceedings of the 31st Photovoltaic Specialists Conference, Lake Buena Vista, FL* (IEEE, New York, 2005), pp. 1343-1345

[3] F. Dreckschmidt, T. Kaden, H. Fiedler, and H.J. Möller, ELECTROLUMINESCENCE INVESTIGANTION OF THE DECORATION OF EXTENDED DEFECTS IN MULTICRYSTALLINE SILICON, *Proceedings of the 22th European Photovoltaic Solar Energy Conference, Milan, Italy*, (2007), pp. 283-286

[4] J. Schmidt, B. Veith, F. Werner, D. Zielke, and R. Brendel, SILICON SURFACE PASSIVATION BY ULTRATHIN Al_2O_3-FILMS AND Al_2O_3/SiN_x STACKS, *Proceedings of the 35th IEEE Photovoltaic Specialists Conference, Honolulu, USA*, 2010, pp. 885-890

[5] S. Herlufsen, J. Schmidt, D. Hinken, K. Bothe, and R. Brendel, Photoconductance-calibrated photoluminescence lifetime imaging of crystalline silicon, *Physica Status Solidi (RRL)*, **2(6)**, (2008), pp. 245-247

[6] D. Hinken, C. Schinke, S. Herlufsen, A. Schmidt, K. Bothe, and R. Brendel, Experimental setup for camera-based measurements of electrically and optically stimulated luminescence of silicon solar cells and wafers, *Review of Scientific Instruments*, **82**, 033706 (2011)

[7] D. V. Lang, Deep - level transient spectroscopy: A new method to characterize traps in semiconductors, *J. Appl. Phys.* **45**, 3023 (1974)

[8] S. Weiss, R. Beckmann, and R. Kassing, The Electrical Properties of Zinc in Silicon, *Appl. Phys. A* **50**, 151-156 (1990)

[9] L.C. Kimerling, and J.L. Benton, ELECTRONICALLY CONTROLLED REACTIONS OF INTERSTITIAL IRON IN SILICON, Physica B **116**, (1983), pp. 297-300